Environment. Technology. Resources. Rezekne, Latvia
Proceedings of the 16th International Scientific and Practical Conference. 2025. Volume IV, 475-480

Optimization of Parameters for White and Dark Laser Marking of Copper and Brass Products

Lyubomir Lazov
Rezekne Academy of Riga Technical University
Rezekne, Latvia
lyubomir.lazov@rta.lv

Risham Singh Ghalot
Rezekne Academy of Riga Technical University
singhrisham93@gmail.com

Nikolay Angelov
Department of Mathematics Informatics and Natural Sciences
Technical University of Gabrovo
Gabrovo, Bulgaria
angelov.np@abv.bg

***Abstract*— This publication examines two principal techniques of fibre laser marking on copper and brass substrates, focusing on the achievement of both dark and white (light) markings. It investigates the effects of marking speed, power density, frequency, and raster pitch on marking contrast. The study identifies the power density threshold that distinguishes between light and dark markings, determining the experimental critical power density for melting at varying speeds for both materials. It also compares experimental values with theoretical predictions of critical melting power density. The findings offer practical recommendations for optimizing laser parameters to achieve high-contrast markings, thereby enhancing traceability and quality control in industrial applications involving copper and brass components.**

***Keywords*— Brass, Contrast, Copper, Fibre Laser, Laser Marking, Power Density, Raster Step, Speed.**

I. Introduction

Laser marking has become an essential technology for the permanent labelling and traceability of metal components across various industries, including electronics, automotive, military production, medical device industry, and aerospace. The ability to create both light and dark markings on copper and brass is particularly valuable for enhancing product identification and quality control. Dark markings provide high contrast for easy visual recognition, while light markings offer subtle, durable labels suitable for automated registration. The capability to achieve both marking types on a single sample opens new possibilities in manufacturing processes.

However, laser marking of copper and brass presents significant challenges due to their high reflectivity and thermal conductivity. These properties make it difficult to achieve consistent contrast and precise control over the marking process [1] – [7]. High reflectivity reduces the absorption of laser energy, with much of it being dissipated into space, while high thermal conductivity of materials leads to heat transfer outside the impact zone, which can lead to the creation of a larger heat-affected zone and deterioration of the marking quality [8] – [10]. These factors complicate the task of achieving the desired marking result and determining the necessary values of power density, marking speed, frequency and raster step.

Several studies have explored laser marking of copper and brass, focusing on aspects such as surface oxidation, microstructure changes, and the influence of laser parameters on marking quality.

In the paper [10], the study is about the influence of speed, raster pitch and power on the roughness and microhardness of the marked areas of copper samples. The experiments were conducted with a fibre laser and a copper bromide laser. The laser power, scan speed and raster pitch were varied to determine their effect on the obtained microhardness and surface roughness. From the experimental data, the speed dependences of the roughness and microhardness for three degrees and two pulse durations for the fibre laser were obtained. The dependence of the roughness and microhardness on the raster pitch for both types of lasers is also shown.

In the paper [11], the authors investigated the influence of pulse duration, power density, speed and linear density of pulses on the depth of marking on brass alloy 260 samples using a fibre laser. They also obtained results on the influence of speed and pulse duration on the path width in laser marking.

In the publication [12], the authors investigate the role of power density of melting and evaporation and speed to realize several laser technological processes on copper samples for a fibre laser and a CuBr laser. A methodology has been developed to determine preliminary operating intervals of power density for different speeds for the laser marking, laser ablation and laser texturing processes. From

Online ISSN 2256-070X
https://doi.org/10.17770/etr2025vol4.8390

theoretical calculations, graphics of the dependences of the critical power density of melting and evaporation on the speed were drawn. Areas where oxidation, melting or evaporation occur were defined. Comparing the theoretical results and the obtained experimental results shows a very good convergence between them for both laser sources.

Researchers have investigated methods for enhancing contrast and durability, but the transition between light and dark markings, as well as the critical melting power density, have not been studied. While theoretical models exist for predicting melting thresholds, experimental validation across different marking speeds and materials has not been reported in other studies.

This article aims to address these gaps by systematically studying the influence of key laser parameters on marking contrast for copper and brass. The purpose is to determine the experimental critical melting power density for different speeds, compare these values with theoretical predictions, and provide practical guidelines for achieving high-contrast laser markings. The findings contribute to refining laser marking techniques, ultimately enhancing the reliability and versatility of marking processes for industrial applications.

II. Materials and Methods

The research conducted is aimed at simultaneously obtaining light and dark laser marking on copper and brass samples. They are implemented with a fibre laser system.

A. Materials

Copper (Cu) is a metal with exceptional high electrical & thermal conductivity, favourable resistance to corrosion (forms a protective oxide layer), great malleability and ductility, and marvellous antimicrobial properties. These properties contribute to its widespread use in industry like - electrical & electronics, defence, construction, transportation, renewable energy facilities, healthcare sanitation, etc.

Whereas brass (CuZn) is a copper-zinc alloy with superb corrosion resistance, excellent malleability & ductility, satisfactory electrical conductivity, and high wear resistance. It has wide applications in the military industry, architecture, jewellery, plumbing parts manufacturing, musical instruments, sculptures, decorations, etc.

B. Laser System

The used laser system is from the ROFIN (Submerged in Coherent.inc) laser manufacturer. The model used is ROFIN powerline F20 laser system. The technical parameters of the laser system are as follows in the Table 1.

TABLE 1 PARAMETERS OF FIBRE LASER SYSTEM USED IN THE RESEARCH.

Parameters	Denotations	Values	Units
Wavelength	λ	1064	nm
Power	P	20	W
Beam Diameter	d	30	µm
Frequency	ν	20 - 50	kHz
Pulse Duration	τ	4 - 200	ns
Scan Speed	v	1 - 20000	mm/s
Pulse Energy	E_p	0.1 - 1	mJ
Focus	f	184	mm

A laser technological system with a fibre laser (see Fig. 1) operating in the near infrared region and in pulsed mode was used. The pulse duration varies over a wide range, and the high frequency provides a large overlap of the pulses in the direction of the laser beam. The laser system is characterized by high positioning accuracy and good repeatability. The laser beam can be moved at a speed varying within very wide limits [13] – [15].

Fig. 1. ROFIN 20 W fibre laser system at Laser Institute of Rezekne Academy of Technology.

B. Experimental Methods

The experiments aim to investigate the influence of speed v and power density q_s factors on obtaining dark and white (light) marking with a fibre laser on copper and brass samples. The frequency and raster step are kept constant for each of the experiments.

To obtain dark and light marking on copper and brass, matrices were designed to conduct the experiments.

- Study of the influence of speed and power density for obtaining dark and light marking on copper

For copper, the matrix consists of processing areas with dimensions 10 mm × 10 mm arranged in 6 rows and 8 columns, with each area corresponding to a different marking speed v and power density q_s (Fig. 2). Copper samples are prepared and fibre laser marking of these 48 areas is performed. After laser marking of the samples, the contrast k_x^* for each marked area is determined.

Contrast k_x^* measurement could be defined as the visual variation of brightness of the laser processed and un-processed area of the substrate. The contrast k_x^* in percent (%) is determined on the reference scale in the relative units or in percent. On the grey scale of the bitmap, each image can be represented as a number between 0 (black) and 255 (white). A reference number N_f is determined with 'Adobe Photoshop' for the image of the surface around the marked area. For a specific grey scale mark image, by means of comparison (when merging it with a reference image), the

corresponding N_x value is measured. The contrast k_x^* is determined by linear interpolation from the expression (1):

$$k_x^* = \frac{N_f - N_x}{N_f} \times 100\% \quad (1)$$

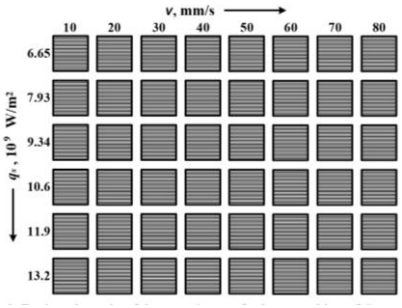

Fig. 2. Designed matrix of the experiments for laser marking of copper samples.

- Study of the influence of speed and power density on obtaining dark and light marking on brass

For brass, the matrix is made of processing areas 5 mm × 5 mm with 3 rows and 7 columns, similar as earlier, with different values of speed v and power density q_s for each area (Fig. 3). Then, marking is performed and the contrast k_x^* of the 21 areas is determined.

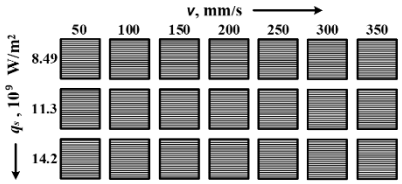

Fig. 3. Designed matrix of the experiments for laser marking of CuZn samples.

- Drawing contrast versus speed graphs and determining critical melting power density for different speeds

For the copper samples, the next step in the study is to plot contrast k_x^* versus speed v for different power densities q_s for light and dark markings. The contrast k_x^* variation intervals for both markings are obtained. The critical power density q_{sc} for melting q_{scm} for different speeds v are determined from the results.

For the brass samples, the contrast k_x^* variation intervals for both types of markings are obtained. The next step is to determine the critical power density q_{sc} for melting q_{scm} for different speeds v.

- Comparison of experimental and theoretical values of critical power density of melting

To compare the experimental q_{scme} and theoretical q_{scmt} values of the critical power density for melting q_{scm}, it is necessary to calculate the theoretical value. It is obtained by the formula (2):

$$q_{scm} = \frac{(1+s)k(T_m - T_0)}{2A}\sqrt{\frac{\pi v}{ad}} \quad (2)$$

where the parameter s is given by the expression $s = \frac{L_m}{c(T_m - T_0)}$, T_m – melting point, T_0 – initial temperature (ambient temperature), A – absorptive capacity, v – speed, a – coefficient of thermal conductivity, d – diameter of the working spot.

III. Results and Discussion

After analysing the marked areas, we found that there is a clear boundary indicating the transition between dark and light marking for different technological parameters – marking speed v, laser power density q_s, raster step Δx and frequency ν. This led us to the idea that the critical power densities q_{sc} for different speeds v at constant values of the other parameters for the selected materials and the technological laser system with a fibre laser can be experimentally determined.

A. Experiments with Copper Samples

According to the designed matrix, laser marking of copper samples was performed. They are for six power densities: $q_{s1} = 6.65 \times 10^9$ W/m^2, $q_{s2} = 7.93 \times 10^9$ W/m^2, $q_{s3} = 9.34 \times 10^9$ W/m^2, $q_{s4} = 10.6 \times 10^9$ W/m^2, $q_{s5} = 11.9 \times 10^9$ W/m^2, and $q_{s6} = 13.2 \times 10^9$ W/m^2, with the speed v varying in the range from 10 mm/s to 80 mm/s in 10 mm/s increments. The parameters that were kept constant during the experiments were: frequency $\nu = 20$ kHz and raster step $\Delta x = 10$ µm. The marked areas are presented in Fig. 4.

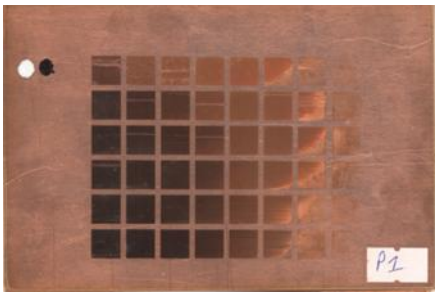

Fig. 4. General view of marked areas on a copper sample.

From the obtained experimental results, graphs of the dependence of contrast k_x^* on speed v for different power densities for dark marking (Fig. 5) and light marking (Fig. 6) are plotted. From them, the following conclusions can be made:

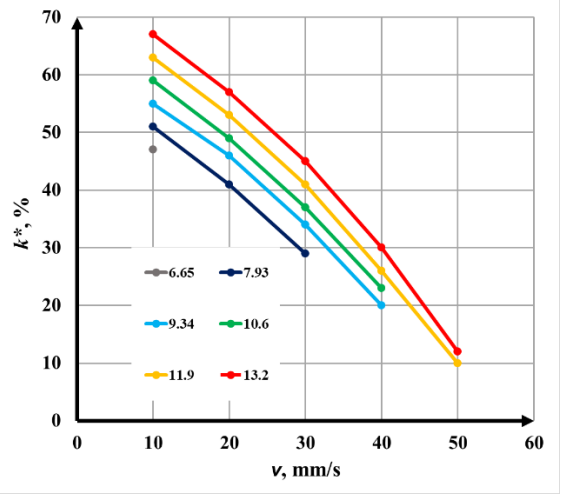

Fig. 5. Graphs of the dependence of contrast on speed for dark marking.

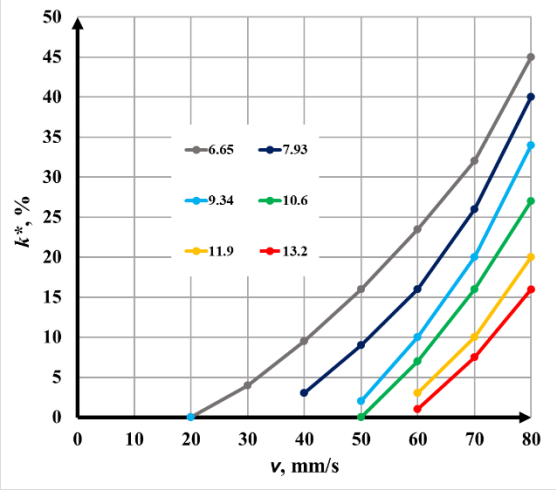

Fig. 6. Graphs of the dependence of contrast on speed for white (light) marking.

- When obtaining a dark marking, the contrast k_x^* varies within the following limits: from 51% to 29% when varying the speed v from 10 mm/s to 30 mm/s and a power density of q_{s2} = 7.93 × 10^9 W/m^2; from 55% to 20% when varying the speed v from 10 mm/s to 40 mm/s and a power density of q_{s3} = 9.34 × 10^9 W/m^2; from 59% to 23% when varying the speed v from 10 mm/s to 40 mm/s and a power density of q_{s4} = 10.6 × 10^9 W/m^2; from 63% to 10% when varying the speed v from 10 mm/s to 50 mm/s and power density of q_{s5} = 11.9 × 10^9 W/m^2 and from 67% to 12% when varying the speed v from 10 mm/s to 50 mm/s and power density of q_{s6} = 13.2 × 10^9 W/m^2.

- For the specified parameters, raster marking is implemented by melting, with the contrast k_x^* changing due to the different roughness of the marked areas [10].

- The following operating speed v intervals were obtained for the visual perception of the dark marking:

- from 10 mm/s to 15 mm/s for q_{s3} = 9.34 × 10^9 W/m^2.
- from 10 mm/s to 18 mm/s for q_{s4} = 10.6 × 10^9 W/m^2.
- from 10 mm/s to 24 mm/s for q_{s5} = 11.9 × 10^9 W/m^2.
- from 10 mm/s to 26 mm/s for q_{s6} = 13.2 × 10^9 W/m^2.

- When receiving a light marking, the contrast k_x^* changes: from 0% to 45% when the speed v varies from 20 mm/s to 80 mm/s and the power density is q_{s1} = 6.65 × 109 W/m2; from 3% to 40% when the speed v varies from 40 mm/s to 80 mm/s and the power density is q_{s2} = 7.93 × 109 W/m2; from 2% to 34% when the speed v varies from 50 mm/s to 80 mm/s and the power density is q_{s3} = 9.34 × 109 W/m2; from 0% to 27% when the speed v varies from 50 mm/s to 80 mm/s and the power density is q_{s4} = 10.6 × 109 W/m2; from 3% to 20% when varying the speed v from 60 mm/s to 80 mm/s and power density is q_{s5} = 11.9 × 109 W/m2 and from 1% to 16% when varying the speed v from 60 mm/s to 80 mm/s and power density is q_{s6} = 13.2 × 109 W/m2.

- This case can be explained by the fact that the resulting laser marking is probably due to oxidation, as the marked surface is lighter than the unmarked surface (the base).

- The following operating speed v intervals were obtained when automatically registering the light marking:

- from 55 mm/s to 80 mm/s for q_{s1} = 6.65 × 10^9 W/m^2.
- from 64 mm/s to 80 mm/s for q_{s2} = 7.93 × 10^9 W/m^2.
- from 70 mm/s to 80 mm/s for q_{s3} = 9.34 × 10^9 W/m^2.
- from 74 mm/s to 80 mm/s for q_{s4} = 10.6 × 10^9 W/m^2.

- The simultaneous obtaining of dark and light marking on one sample allowed us to determine the limit for obtaining laser marking by melting or by oxidation for the selected parameters of the study for fibre laser and material copper, i.e. to determine the experimental critical power density q_{sc} for different speeds v. The results are presented in Table 2. The theoretical values of the critical power density q_{sc} were calculated by formula (2). The comparison between the two values showed that the theoretical values are higher than the experimental ones for the interval of studied speeds v. This result is explained by the fact that the change in the characteristics of copper with increasing temperature during the implementation of the process was not considered in the theoretical calculations.

TABLE 2 EXPERIMENTAL AND THEORETICAL CRITICAL POWER DENSITY FOR MELTING FOR DIFFERENT RATES FOR CU SAMPLES.

v, mm/s	q_{scme}, W/m^2	q_{scmt}, W/m^2
20	6.65 × 10^9	6.79 × 10^9
31	7.93 × 10^9	8.45 × 10^9
43	9.34 × 10^9	9.67 × 10^9
50	10.6 × 10^9	11.3 × 10^9
54	11.9 × 10^9	12.4 × 10^9
58	13.2 × 10^9	13.6 × 10^9

B. Experiments with Brass Samples

The brass samples were exposed to the environment for a long time and had an oxide layer. Their background is changed in this way, which darkens. Experiments were conducted for raster laser marking of a brass sample for three power densities: q_{s7} = 8.49 × 10^9 W/m^2, q_{s8} = 11.3 × 10^9 W/m^2, and q_{s9} = 14.4 × 10^9 W/m^2. The speed v varied from 50 mm/s to 350 mm/s in 50 mm/s increments. The parameters that were kept constant during the experiments were: frequency ν = 100 kHz and raster step Δx = 30 µm. A panoramic photograph of the marked areas is given in Fig. 7. The contrast k_x^* of the marking was determined for each marked square.

Fig. 7. General view of marked areas on a sample of brass.

After analysing the obtained results, the following was established:

- For a power density of q_{s7} = 8.49 × 10^9 W/m^2, a bright marking is obtained for the speed v interval studied as the contrast k_x^* varies from 12% to 75%, and no dark marking is observed. For a power density of q_{s8} = 11.3 × 10^9 W/m^2, a dark marking is available for a speed v of 50 mm/s as the contrast k_x^* is 25%, and a bright marking is obtained for a speed v of 100 mm/s to 350 mm/s as the contrast k_x^* varies from 0 to 43%. For a power density of q_{s9} = 14.4 × 10^9 W/m^2, a dark mark is obtained for a speed v of 50 mm/s to 100 mm/s as the contrast k_x^* varies from 35% to 14%, and a bright mark is obtained for a speed v of 150 mm/s to 350 mm/s as the contrast k_x^* varies from 0 to 27%.

- The dark marking was obtained by removing the oxide layer and subsequent melting of the material (see marked area in left part of Fig. 7). The laser marking process by melting was implemented.

- The light marking was obtained by removing the oxide layer. In these experiments, a light marking is present in most of the investigated speed v interval. It is explained by the fact that a lower power density (lower absorbed energy, respectively) is required to remove the thin oxide layer from the brass sample in the impact zone. At this raster step, the scanning overlap coefficient has a value of 0 ($k_{soc} = 1 - \frac{\Delta x}{d}$), i.e. there is no overlap, as in raster marking the paths touch each other. In addition, the used frequency of 100 kHz gives a lower pulse energy ($E_p = \frac{P}{\nu}$). The combination of high-speed v, low power density, low pulse energy and zero scanning overlap coefficient do not allow the melting of the brass sample after removing the oxide layer.

- Again, as with the copper sample, simultaneous dark and light markings were obtained on the brass sample. This allowed the determination of the critical power density for melting q_{scm} for two speeds v. The experimental and theoretical results are given in Table 3. Comparing the theoretical values of the critical power density q_{sc} with the experimental ones for both speeds v shows that the theoretical values are higher than the experimental ones.

Experimental determination of critical power densities q_{sc} provides guidance for determining the power density q_s and speed v intervals when conducting research for a specific marking method, for example by oxidation, layer removal (nickel-plated, galvanized, etc. sample) and melting. This shortens the time from the research process to the implementation in production of the laser marking process on products.

TABLE 3 EXPERIMENTAL AND THEORETICAL CRITICAL POWER DENSITY FOR MELTING FOR DIFFERENT RATES FOR CUZN SAMPLES.

v, mm/s	q_{scme}, W/m^2	q_{scmt}, W/m^2
100	11.3 × 10^9	11.7 × 10^9
150	14.4 × 10^9	14.2 × 10^9

C. QR Code marking on Copper and Brass Samples

Quick Response (QR) codes with dimensions ranging between 3 mm to 4 mm were obtained on copper & brass samples with dark and light markings through the optimal research results. The values of the parameters are as follows:

a) QR codes on copper surface (Fig. 8)

- For dark marking, the power density is q_{s5} = 11.9 × 10^9 W/m^2, v = 20 mm/s and ν = 20 kHz.
- For light marking, the power density is q_{s5} = 11.9 × 10^9 W/m^2, v = 80 mm/s and ν = 20 kHz.
- A laser marked QR code of size 3.5 mm, in light marking, was scannable with an electronic device.

Fig. 8. Obtained QR codes on copper surface – starting from left end, white (light) and dark marking, respectively.

b) QR codes on brass surface (Fig. 9)

- For dark marking, the power density is q_{s9} = 14.4 × 10^9 W/m^2, v = 50 mm/s and ν = 100 kHz.

- For grey marking, the power density is q_{s8} = 11.3 × 10^9 W/m^2, v = 50 mm/s and ν = 100 kHz.
- For light marking, the power density is q_{s7} = 8.49 × 10^9 W/m^2, v = 200 mm/s and ν = 100 kHz.
- A laser marked QR code of size 3.8 mm, in light marking, was scannable with an electronic device.

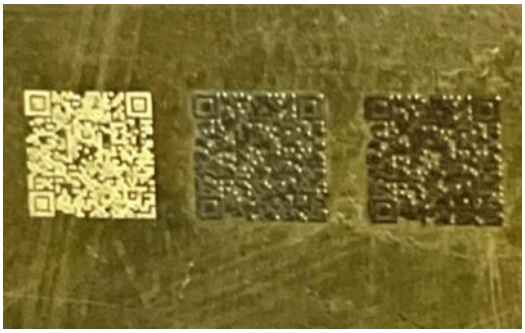

Fig. 9. Obtained QR codes on brass surface – starting from left end, white (light), grey (middle) and dark (right end) marking, respectively.

IV. Conclusions

This publication concerns the influence of some technological parameters for obtaining dark and light marking with a fibre laser simultaneously on one sample for the materials copper and brass. The influence of marking speed, power density, frequency and raster pitch on the contrast k_x^* of the marking is studied. The following results have been achieved:

- Working speed intervals for different power densities for obtaining dark and light marking on copper samples have been determined.
- Working speed intervals for different power densities for obtaining dark and light marking on brass samples have been determined.
- The experimental value of the critical melting power density for different speeds for the two materials has been determined based on finding the limit for obtaining light or dark marking.
- A comparison has been made between the experimental and theoretical values of the critical power density of melting for different speeds.
- Light and dark markings of QR codes have been obtained using optimal technological parameters from the studies.

These results will help to deepen the knowledge of the laser marking process of copper and brass products and the application of these two types of marking in production conditions.

References

[1] N. G. Henriksen, O. Z. Andersen, M. S. Jellesen, T. L. Christiansen and M. A. Somers, "Influence of Laser Marking on Microstructure and Corrosion Performance of Martensitic Stainless-Steel Surfaces for Biomedical Applications, " HTM Journal of Heat Treatment and Materials, vol. 77, no. 3, pp. 177-196, 2022, https://doi.org/10.1515/htm-2022-1010

[2] A. Syakila, M. Jamaludin, M. Quazi, M. Aiman and A. Arslan, Eds., Effect of Laser Parameters on Colour Marking of Ti6Al4V Titanium Alloy, 7th International Conference on Mechanical Engineering Research 2023 (ICMER 2023), Journal of Physics: Conference Series 2688 (2024) 012009, 2024, DOI: 10.1088/1742-6596/2688/1/01200910

[3] K. Kanev, P. Gnatyuk and V. Gnatyuk, "Laser Marking in Digital Encoding of Surfaces," Advanced Materials Research, Vol. 222, pp 78-81, 2021, doi:10.4028/www.scientific.net/AMR.222.78

[4] L. Morawiński, S. Świłło and A. Kocań, Eds., Application of Laser Barcode Technology to Sheet Metal Parts Identification, Scientific Papers of Silesian University of Technology, Organization and Management Series, No. 162, pp. 501-516, 2022, http://dx.doi.org/10.29119/1641-3466.2022.162.27

[5] L. Sobotova and M. Badida, "Laser marking as environment technology, " Open Engineering, 7(1), pp. 303-316, November 2017, DOI: https://doi.org/10.1515/eng-2017-0030

[6] C. Leone, E. Bassoli, S. Genna and A. Gatto, "Experimental investigation and optimization of laser direct part marking of Inconel 718," Optics and Lasers in Engineering, Vol. 111, pp. 154-166, 2018, https://doi.org/10.1016/j.optlaseng.2018.08.004

[7] C. Velotti, A. Astarita, C. Leone, S. Genna, F. Minutolo and A. Squillace, Eds., Laser marking of titanium coating for aerospace applications, Procedia CIRP, Vol. 41, pp. 975-980, 2016, https://doi.org/10.1016/j.procir.2016.01.006

[8] V. Jurčs, E. Yankov, N. Angelov, A. Pacejs and I. Adijāns, Eds., Influence of Technological Parameters on Laser Marking Process of Copper Surfaces, Environment. Technology. Resources. Rezekne, Latvia Proceedings of the 15th International Scientific and Practical Conference. Volume III, pp. 393-398, DOI: https://doi.org/10.17770/etr2024vol3.8179

[9] J. Hlinka and Z. Weltsch, Eds., Analysis of Laser Treated Copper Surfaces, Periodica Polytechnica Transportation Engineering, 47(2), pp. 140-145, 2018, DOI: 10.3311/PPtr.11561

[10] R. Ghalot, l. Lazov, E. Yankov, N. Angelov, "Investigation of the Change in Roughness and Microhardness during Laser Surface Texturing of Copper Samples by Changing the Process Parameters, " Coatings, 13, no. 11, 1970, 2023, https://doi.org/10.3390/coatings13111970

[11] D. Klavins, L. Lazov, A. Pacejs, R. Revalds and E. Zaicevs, Eds., Research of Laser Marking and Engraving on Brass Alloy 260, Proceedings of the 12th International Scientific and Practical Conference: Environment. Technology. Resources, 2019, DOI:10.17770/etr2019vol3.4167

[12] R. Ghalot, L. Lazov, N. Angelov and E. Teirumnieks, Eds., Determination of Preliminary Operating Intervals of Power density for Laser Technological Processes on Copper Samples, Environment Technology Resources: Proceedings of the 15th International Scientific and Practical Conference, Rezekne, 2024, https://doi.org/10.17770/etr2024vol3.8180

[13] "Coherent," [Online]. Available: www.coherent.com. [Accessed 2020].

[14] M. Zervas and C. Codemard, "High Power Fiber Lasers: A Review, " IEEE Journal of Selected Topics in Quantum Electronics, vol. 20, no. 5, 0904123, 2014, DOI: 10.1109/JSTQE.2014.2321279

[15] Duarte F., Tuneable Laser Applications, 3rd ed., CRC Press, 2016, pages 452, ISBN:9781482261073.